Switching Spin and Charge between Edge States in Topological Insulator Constrictions

Viktor Krueckl and Klaus Richter

Institut für Theoretische Physik, Universität Regensburg, D-93040 Regensburg, Germany

(Received 14 May 2011; published 17 August 2011)

We show how the coupling between opposite edge states, which overlap in a constriction made of the topological insulator mercury telluride (HgTe), can be employed both for steering the charge flow into different edge modes and for controlled spin switching. Unlike in a conventional spin transistor, the switching does not rely on a tunable Rashba spin-orbit interaction, but on the energy dependence of the edge state wave functions. Based on this mechanism, and supported by extensive numerical transport calculations, we present two different ways to control spin and charge currents, depending on the local gating of the constriction, resulting in a high fidelity spin transistor.

DOI: 10.1103/PhysRevLett.107.086803 PACS numbers: 73.23.−b, 85.35.Ds, 85.75.Hh

Since the prediction of a new topological state of matter in graphene [1], materials exhibiting peculiar surface states and acting as topological insulators have attracted wide attention [2]. Shortly after the theoretical proposal for a mercury telluride (HgTe)-based two-dimensional topological insulator [3,4], the observation of the quantum spin Hall effect [5] and nonlocal edge transport [6] brought compelling experimental evidence for quantized conductance due to edge states. The transport along the HgTe boundaries can be conveniently explained by an edge channel picture [7]: Two states with opposite spin orientation propagate along opposite device edges in the same direction and thus lead to a quantized conductance of $2e^2/h$. Because of the spatial separation of the spin states the spin-orbit coupling is suspended, and the system geometry can be employed for spin selection [6].

Spin selectivity is also a crucial element of the Datta-Das spin-transistor proposal [8], where charge flow is controlled electrically through the gate-dependent Rashba spin-orbit interaction (SOI) [9] in a conventional two-dimensional semiconductor heterostructure placed in between ferromagnetic contacts. Its realization, however, turns out to be difficult owing to spin relaxation in the semiconductor heterostructure and interfacial effects such as the conductivity mismatch [10] between the different materials. HgTe-based topological insulators appear to be promising candidates for spin processing devices since they also can be gated and exhibit considerable SOI but, on the contrary, are composed of a single material class only. Moreover, the one-dimensional nature of their edge states suppresses orbital effects present in bulk conductors, leading to high spin polarizations and to a much better (spin) switching quality.

To our knowledge there have been only a few proposals for spin transistors based on two-dimensional topological insulators. Two of them rely on spin switching with a magnetic field at a *p-n* junction [11] or in an Aharonov-Bohm interferometer [12]. Recently it has further been suggested, also within a phenomenological model, that separate gating of the two branches of an Aharonov-Bohm interferometer allows for manipulating charge and spin transport [13]. In contrast, our present proposal relies on an electrical operation by gates on a single HgTe constriction, which up to now has only been considered for charge current switching [14].

In this Letter we demonstrate how topological edge states can be selectively switched in an elongated constriction etched out of a HgTe heterostructure, leading to an integrated three-state charge and spin transistor of high fidelity. An incoming spin-polarized (upper edge) state can either be reflected back to the lower edge, as shown in Fig. 1(a), or transmitted through the narrow part. Backreflection into the opposite spin channel at the same edge is forbidden, as the absence of a magnetic field implies time-reversal symmetry [2]. Within the constriction the SOI between the edge channels is reactivated due to a finite overlap between right moving edge states on the upper and the lower sides, giving rise to spin precession that is tunable by a gate. This allows for steering the spin orientation of the electrons which leave the constriction, and thereby their further path: An incoming spin-up state will leave the system either by swapping the edge (with a simultaneous spin flip), as shown in Fig. 1(b), or by remaining in its spin and edge state as shown in Fig. 1(c). Furthermore, employing numerical quantum transport calculations, we analyze the peculiar switching properties by means of a top gate and side gates acting on the constriction.

We describe the electronic properties of the underlying HgTe heterostructure by the four-band Hamiltonian [3,6]

$$H = \begin{pmatrix} C_k + M_k & Ak_+ & -iRk_- & -\Delta \\ Ak_- & C_k - M_k & \Delta & 0 \\ iRk_+ & \Delta & C_k + M_k & -Ak_- \\ -\Delta & 0 & -Ak_+ & C_k - M_k \end{pmatrix}, \quad (1)$$

where $k_\pm = k_x \pm ik_y$, $\boldsymbol{k}^2 = k_x^2 + k_y^2$, $C_k = -D\boldsymbol{k}^2$, and $M_k = M - B\boldsymbol{k}^2$. This Hamiltonian contains the commonly

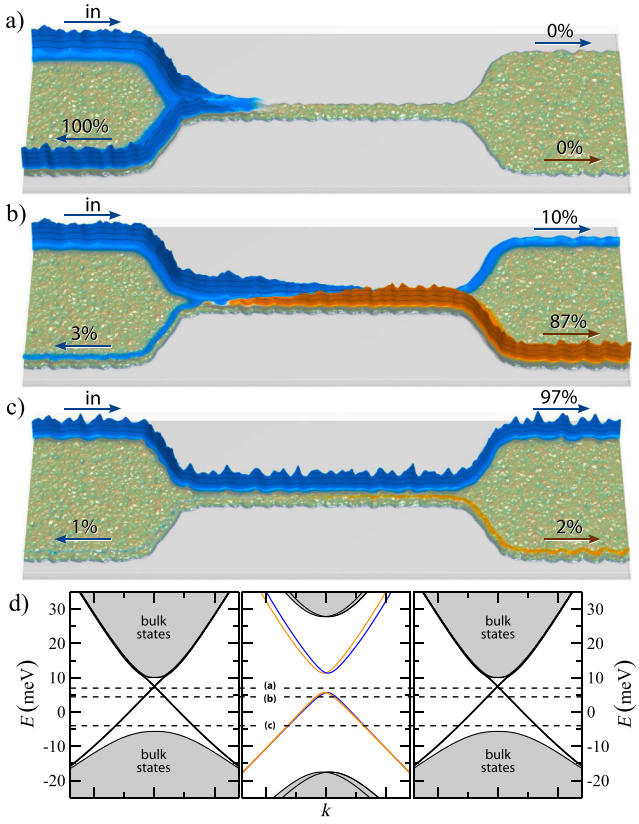

FIG. 1 (color online). Spin-resolved local density of states for charge carriers entering a constriction from the upper left edge. Color code indicates spin polarization [dark gray (blue) ($\uparrow$), light gray (orange) ($\downarrow$)]. (a) Perfect reflection of the incoming state for a chemical potential within the confinement induced gap [$\mu = 7$ meV, upper dashed line in (d)]. (b) For an energy closely below the gap ($\mu = 4$ meV), considerable SOI results in a spin flip associated with a switching between the edges. (c) Energy distinctly below the gap ($\mu = -5$ meV), leads to a reduced effective SOI, and hence the spin state leaves the constriction unrotated. (d) Sketch of the band structure for a sequence of a wide (left panel, $W = 1000$ nm), narrow (middle panel, $W = 100$ nm), and wide (right) lateral confinement.

used time-inverted 2×2 blocks for the composite states of the heavy hole and electron bands [3]. Additionally, we take into account the leading order SOI terms Δ and R, due to bulk-inversion asymmetry and structure-inversion asymmetry [15], respectively (for material parameters in Eq. (1), see Supplemental Material [16]).

Based on the Hamiltonian (1) we first derive an effective model Hamiltonian for an infinite strip of constant width W. We chose the lead to point in the x direction and search for the transversal eigenfunctions $\psi(y)$ which separately fulfill the boundary conditions $\psi(y \leq 0) = 0$ at the lower side and $\psi(y \geq W) = 0$ at the upper side. For a very wide confinement one can neglect the influence of the opposite boundary on the edge states, leading to a full spin polarization. Then the resulting states can be classified by their subblock into up ($\uparrow$) and down ($\downarrow$), as well as their propagation direction into right movers ($+$) and left movers ($-$). Accordingly, the right moving states of the upper and lower subblock are given by

$$\psi_{\uparrow}^{+}(y) \propto (e^{\lambda_1^+(y-W)} - e^{\lambda_2^+(y-W)})(1, -\xi^+, 0, 0), \quad (2)$$

$$\psi_{\downarrow}^{+}(y) \propto (e^{-\lambda_1^+ y} - e^{-\lambda_2^+ y})(0, 0, 1, \xi^+), \quad (3)$$

with two different decay exponents λ_1^+, $\lambda_2^+ > 0$, and ξ^+ the weight of the second spinor entry in the respective subblock. The left moving states are obtained by complex conjugation and by substituting $y \rightarrow W - y$ and $k_x \rightarrow -k_x$ [16]. From these properties we can derive an effective 1D Dirac Hamiltonian $H_{\text{eff}\uparrow/\downarrow} = c \mp a\sigma_x k_x$ for a single spin subblock with a velocity $a = A\sqrt{(B^2 - D^2)/B^2}$ and an energy offset $c = -DM/B$. For a wide strip this is in perfect agreement with the full band structure in the vicinity of the band crossing shown in the left and right panels of Fig. 1(d) for $W = 1000$ nm.

For decreasing width W, the edge states at opposite boundaries start to overlap, leading to a masslike gap in the 1D Hamiltonian. By invoking simultaneously the boundary conditions for the upper and lower sides the size of the effective mass gap is given by [17]

$$m \approx \frac{2|A(B^2 - D^2)M|}{B^3(A^2B - 4(B^2 - D^2)M)} e^{-\lambda_1^+ W}. \quad (4)$$

Additionally, the suppression of the SOI for distant edge states is suspended for small W. Neglecting the rapidly decaying terms proportional to $e^{\lambda_2^{\pm} y}$ in the wave function, the overlap due to bulk-inversion asymmetry can be stated as

$$\delta^{\pm} \approx -\frac{4e^{-\lambda^{\pm} W}\lambda^{\pm} W \xi^{\pm}}{1 + (\xi^{\pm})^2}\Delta. \quad (5)$$

The effect of structure-inversion asymmetry on the edge states within the band gap is negligible small. Combining m of Eq. (4) and the effective SOI $\delta^{\pm}$ of Eq. (5), we can compose a 1D effective Hamiltonian

$$H_{\text{eff}} = \begin{pmatrix} c + m & -ak_x & \delta_m & \delta_p \\ -ak_x & c - m & -\delta_p & -\delta_m \\ \delta_m & -\delta_p & c + m & ak_x \\ \delta_p & -\delta_m & ak_x & c - m \end{pmatrix}, \quad (6)$$

with $\delta_{p/m} = (\delta^+ \pm \delta^-)/2$. The band structure of H_{eff} shows a mass gap and an energy-dependent effective spin-orbit splitting which is strongest close to the avoided band crossing shown in the middle panel of Fig. 1(d). Note that the SOI of this model is slightly overestimated compared to the result of the full Hamiltonian (1).

In the following, we analyze within this 1D model [18] the transport properties for a constriction interconnecting two bulklike regions in an H-shaped HgTe heterostructure, as depicted in Fig. 2(a). Within the bulk band gap the transport is exclusively carried by edge states.

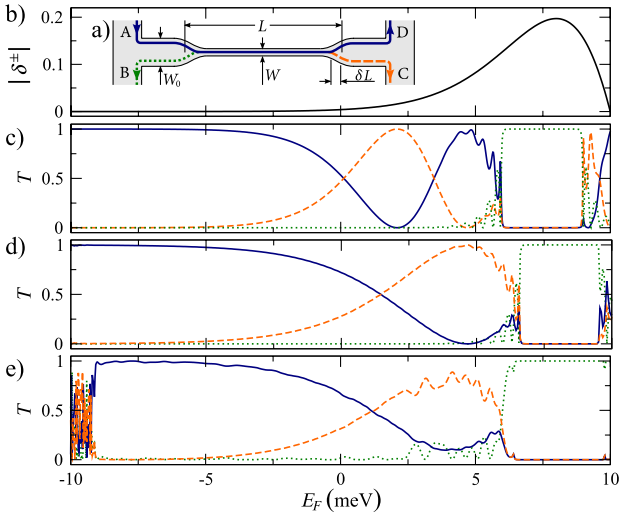

FIG. 2 (color online). (a) Sketch of the constriction geometry. Colored paths illustrate the differently scattered edge channels leaving the system at lead B (green dotted line), C (orange dashed line), or D (blue solid line). (b) Energy dependence of the effective SOI, Eq. (5). (c) Transmission through a constriction calculated by means of the 1D model Hamiltonian (6). (d), (e) Transmission obtained by a full numerical wave-packet calculation for (d) a perfect constriction and (e) a realistic constriction with random impurity potential ($U_0 = 2$ meV) and rough walls ($W_r = 20$ nm), the same system as used in Figs. 1(a)–1(c). Geometric properties of the constriction are width $W = 100$ nm, length $L = 1900$ nm ($\delta L = 50$ nm), width of bulk parts $W_0 = 1000$ nm.

Accordingly, there are three different paths entering at lead A and leaving the system at lead B (green dotted line), C (orange dashed line), or D (blue solid line). Neglecting SOI this setting equals a Dirac equation with a position-dependent mass potential, which can be solved analytically for an abrupt change in W [19] leading to strong Fabry-Pérot-like transmission resonances for energies outside the confinement induced gap. Here we use a smooth transition (on a scale δL) between the width W_0 outside and the width W inside the constriction (of length L) given by

$$W(x) = W_0 - \left(\frac{W_0 - W}{1 + e^{(x-L/2)/\delta L}} - \frac{W_0 - W}{1 + e^{(x+L/2)/\delta L}}\right); \quad (7)$$

see Fig. 2(a). W_0 is chosen wide enough to ensure a gapless Dirac spectrum. With SOI the right moving spin-up and spin-down states hybridize within the constriction to a symmetric and an antisymmetric composite state with a difference in the wave vectors of $\Delta k \approx |\delta^+|/a$. Since the overlap strongly depends on the extent of the edge states $\propto e^{-\lambda_1^{\pm} y}$, the effective spin-splitting energy $|\delta^{\pm}|$ [in Eq. (5)] has a pronounced energy dependence as shown in Fig. 2(b). For low energies (larger $\lambda_1^{\pm}$) both states are very closely bound to opposite edges. Thus the effective SOI is very weak and the states preserve their initial spin while traveling through the constriction [see also Fig. 1(c)], leading to a perfect transmission from lead A to D as shown by the solid blue curve in Fig. 2(c). At higher energies the spin splitting is pronounced [see Fig. 2(b) and also the band structure in Fig. 1(d)]; hence, the states undergo a spin precession when traversing the constriction and leave the device at lead C. For even higher energies in the mass gap, the transmission is blocked leading to a reflection along path B. Note that the three different transmission probabilities displayed in Fig. 2(c) show well separated and pronounced maxima up to unity for the various paths. The different switching states span at least an energy range of 2 meV; thus, the effect survives a few tens of Kelvin. As a result the 1D model suggests that a HgTe constriction is perfectly suited to function as a three-state spin-orbit transistor, switching with excellent on-off ratio between the outgoing leads B, C, and D. At the same time, this system allows for controlled spin swapping, i.e., when choosing path A to C.

In the following we study the robustness of these effects for a realistic setting, governed by the two-dimensional four-band Hamiltonian (1) with additional random impurity potentials and rough walls. We have extended an efficient numerical method to calculate electronic transport by means of the time evolution of wave packets [20] to arbitrary spin-orbit coupled systems. The propagation is calculated by means of an expansion of the time-evolution operator in Chebychev polynomials [21], ensuring negligible numerical errors for long propagation times [22]. We add an impurity potential with $U_0 = 2$ meV and a wall roughness of $W_r = 20$ nm [16].

The resulting energy-dependent transmissions for a clean and a disordered system are summarized in Figs. 2(d) and 2(e). Because of impurity induced energy variations within the constriction and fluctuations in its width, the mass gap is enhanced. Most notably, the strength of the spin-flip mechanism is maintained compared to a calculation without disorder, although the efficiency of the spin-flip process is slightly reduced by the impurity potential and the wall roughness: The spin-flip transmission [from lead A to C, dotted orange line in Fig. 2(e)] no longer reaches $T = 1$ [see also Fig. 1(b)]. Nevertheless, this reduction only amounts to 20% for a very strong perturbation as used in these calculations. Consequently, we conclude that the switching properties of such a device are robust against electrostatic impurities and persist in nonperfectly etched heterostructures.

In the following we consider the possibility of controlled switching between edge currents by an additional gate. We model local gating that has been proven experimentally feasible [6], by a position-dependent potential which is switched on outside of the confined region [see Fig. 3(a)]. Furthermore, a random impurity potential as well as edge roughness are again considered, as specified above. By means of our wave packet algorithm we calculate the quantum transport through the device as a function of

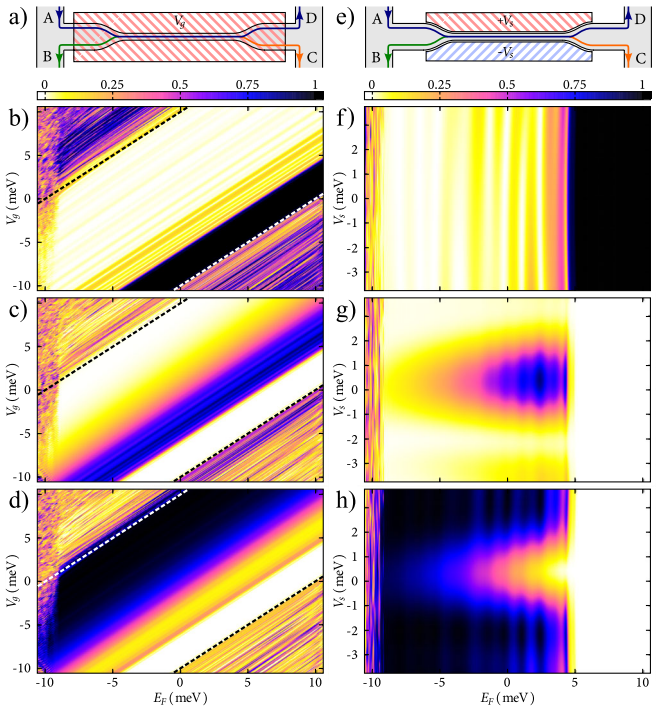

FIG. 3 (color online). (a) Scheme of the constriction (width $W = 100$ nm, length $L = 1900$ nm) coupled to bulk parts (width $W_0 = 1000$ nm) and subject to a top gate (red hatched area). A random potential with $U_0 = 2$ meV and wall roughness of $W_r = 20$ nm are included as visualized in Figs. 1(a)–1(c). Panels (b)–(d) show the (color coded) quantum transmission from lead A to the lead B (b), C (c), and D (d) as a function of the Fermi energy E_F and the top-gate voltage V_g. (e) Scheme of a smaller constriction ($W = 60$ nm, $W_r = 10$ nm, $L = 900$ nm, $W_0 = 1000$ nm) with two side gates. (e), (f) Transmission from lead A to lead B (f), C (g), and D (h) as a function of E_F and side-gate voltage V_s. Panels (b)–(d) and (f)–(h) feature a spin-transistor switching.

both Fermi energy and gate voltage. The resulting transmissions into leads B to D are shown in Figs. 3(b)–3(d), where large (small) transmissions are depicted by dark (bright) colors. Note that all plots show universal conductance fluctuations for energies outside the bulk band gap [marked by dashed lines in Figs. 3(b)–3(d) and given approximately by $E_F - V_g < -|M|$ and $E_F + V_g > |M|$]. Within the bulk band gap the device exhibits the switching properties. The Fermi energy within the whole system is pinned to a certain value and can be globally tuned, e.g., by means of another back gate. Assuming for example $E_F = 0$, the transmission can be steered between the three different leads by changing the gate voltage and thereby changing the energy-dependent effective SOI shown in Fig. 2(b) (contrary to the Datta-Das proposal [8] based on tuning the Rashba SOI). In this case a perfect transmission to lead B is achieved for $V_g = -7$ meV. For $V_g = -4$ meV the transmission to lead C is maximal, whereas for $V_g = 5$ meV the transmission to lead D approaches unity.

A similar effect occurs when we use two side gates close to the constriction with an opposite applied voltage V_s, as sketched in Fig. 3(e). This leads to different chemical potentials for the two spin channels close to the upper and lower sides of the constriction. The results of a corresponding conductance calculation are summarized in Figs. 3(f)–3(h). Because of the different gating, the mass gap now shows up as a vertical stripe ($E_F > 5$ meV), and the constriction is isolating, independent of the gate voltage V_s, as shown in Fig. 3(f). If the constriction is tuned into the state conducting charge from left to the right ($E_F < 5$ meV), it works as a spin transistor controlled through the side-gate voltage V_s: For low $|V_s|$ the states entering the device undergo a spin flip within the constriction, whereas for larger $|V_s|$ the momenta of different spin states differ sufficiently to suppress the spin precession. The calculations [3(f)–3(h)] were performed for a narrower constriction ($W = 60$ nm) and the same amount of disorder to demonstrate that the switching functionality is robust against down scaling to a regime of a few 10 nm. In view of Eq. (5), the effective SOI increases with decreasing width, allowing for faster spin precession and shorter constrictions (see [16]).

To summarize, we have shown that a constriction joining together edge channels of the topological insulator HgTe acts as a transistor with unique charge and spin switching properties. These are robust against disorder and edge roughness as present in experiments. Mediated through an effective spin-orbit coupling arising in the constriction, a local top gate enables switching between the edge states, while side gates allow for pure spin-transistor action. Such constrictions may serve as building blocks and connectors for more complex spin- and charge-selective edge channel networks based on topological insulators.

This work is supported by Deutsche Forschungsgemeinschaft (GRK 1570 and joined DFG-JST Forschergruppe Topological Electronics). We thank H. Buhmann, M. Wimmer, and J. Wurm for useful conversations and M. Krueckl, J. Kuipers, and M. Wimmer for a careful reading of the manuscript.

[1] C. L. Kane and E. J. Mele, Phys. Rev. Lett. **95**, 146802 (2005); Phys. Rev. Lett. **95**, 226801 (2005).
[2] M. Z. Hasan and C. L. Kane, Rev. Mod. Phys. **82**, 3045 (2010).
[3] B. A. Bernevig, T. L. Hughes, and S.-C. Zhang, Science **314**, 1757 (2006).
[4] B. A. Bernevig and S.-C. Zhang, Phys. Rev. Lett. **96**, 106802 (2006).
[5] M. König *et al.*, Science **318**, 766 (2007).
[6] A. Roth *et al.*, Science **325**, 294 (2009).
[7] M. Büttiker, Phys. Rev. B **38**, 9375 (1988).
[8] S. Datta and B. Das, Appl. Phys. Lett. **56**, 665 (1990).
[9] Y. A. Bychkov and E. I. Rashba, JETP Lett. **39**, 78 (1984).
[10] G. Schmidt *et al.*, Phys. Rev. B **62**, R4790 (2000).

[11] A. R. Akhmerov, C. W. Groth, J. Tworzydło, and C. W. J. Beenakker, Phys. Rev. B **80**, 195320 (2009).
[12] J. Maciejko, E.-A. Kim, and X.-L. Qi, Phys. Rev. B **82**, 195409 (2010).
[13] F. Dolcini, Phys. Rev. B **83**, 165304 (2011).
[14] L. B. Zhang, F. Cheng, F. Zhai, and K. Chang, Phys. Rev. B **83**, 081402 (2011).
[15] D. G. Rothe *et al.*, New J. Phys. **12**, 065012 (2010).
[16] See Supplemental Material at http://link.aps.org/supplemental/10.1103/PhysRevLett.107.086803 for material parameters, relation between spin precession and channel width, wave packet algorithm, and details of the impurity and rough edge model.
[17] B. Zhou *et al.*, Phys. Rev. Lett. **101**, 246807 (2008).
[18] A similar model in terms of a spinful Luttinger liquid coupled to two helical ones was recently studied in C.-X. Liu, J. C. Budich, P. Recher, and B. Trauzettel, Phys. Rev. B **83**, 035407 (2011).
[19] J. V. Gomes and N. M. R. Peres, J. Phys. Condens. Matter **20**, 325221 (2008).
[20] T. Kramer, C. Kreisbeck, and V. Krueckl, Phys. Scr. **82**, 038101 (2010).
[21] H. Tal-Ezer and R. Kosloff, J. Chem. Phys. **81**, 3967 (1984).
[22] V. Krueckl and T. Kramer, New J. Phys. **11**, 093010 (2009).